Journal of the European Ceramic Society **15** (1995) 769–775
© 1995 Elsevier Science Limited
Printed in Great Britain. All rights reserved
0955-2219/95/$9.50

0955-2219(95)00045-3

Mechanical Properties of a Partially Sintered Alumina

Dale Hardy & David J. Green

Department of Materials Science and Engineering, The Pennsylvania State University, University Park, PA 16802, USA

(Received 8 June 1994; revised version received 10 February 1995; accepted 14 February 1995)

Abstract

An experimental investigation was performed to understand the mechanical properties of alumina with moderate amounts of porosity (~20–40%). Young's modulus, strength and fracture toughness showed similar behavior as a function of the degree of sintering. For low sintering temperatures (<1050°C), the mechanical properties were found to change significantly with only minimal densification, and this was considered to be due to neck growth by surface diffusion. At these temperatures, increases in sintering time resulted in further increases in Young's modulus. The Young's modulus and fracture toughness data agreed well with modifications to a recent theory. The critical crack size in these porous materials calculated from the strength and fracture toughness data was found to increase slightly as the sintering temperature was increased. It was concluded that significant improvements in the mechanical properties of porous ceramics can be obtained by control of the sintering process, and in some cases these improvements can be made with minimal densification.

1 Introduction

There are many technological applications in which porous ceramic materials are utilized. For example, high-porosity cellular ceramics can be used for molten-metal filters, radiant burners, lightweight cores for sandwich panels, etc. In other cases, ceramics with moderate amounts of porosity are needed, e.g. as particle filters, catalyst supports and sensors. For structural components, the presence of porosity may be useful in reducing the weight of the component, whereas for non-structural components, porosity may be essential for other functions, such as permeability or a high-surface-area substrate. For both structural and non-structural applications, however, improvements in the mechanical properties and control of strength variability are expected to increase the overall reliability of the material. In order to accomplish this goal, the interrelationship between processing, structure and mechanical properties of porous materials must be understood. The most common way of processing moderately porous ceramic materials is by sintering powder compacts to a fixed degree of densification. During this process, the particles coalesce by the formation of necks, and the particles usually undergo grain coarsening and other geometric changes. The aim of the current study was to measure the room-temperature mechanical properties of a partially sintered alumina, i.e. Young's modulus, fracture toughness and strength, and relate these properties to the sintering process.

2 Background

In order to understand the effect of porosity on mechanical properties, researchers have usually emphasized the volume fraction and geometry of the porosity. In some recent studies,[1–7] however, there has been an attempt to relate the mechanical properties to the microstructure of the *solid* phase, linking the properties to neck growth, particle coordination, solid phase contiguity, etc. Green and coworkers[2,6] have demonstrated a dramatic increase in the strength and elastic moduli of alumina with no change in pore volume. This sharp increase in stiffness with minimal increase in density was attributed to neck growth by surface diffusion, the dominant mechanism in the sintering of alumina at temperatures below ~1000°C. Using a simple model for the initial stages of neck growth that emphasizes the solid microstructure, Green *et al.* suggested[1,2]

$$(B/B_0) = [3Nr(1-2\nu_0)]/[8kR(1-\nu_0^2)] \quad (1)$$

where B is the bulk modulus of the porous compact, B_0 and ν_0 are the bulk modulus and Poisson's ratio of the particle, r is the neck radius, N is the particle coordination number, R is the radius of the particle and k is a geometric constant. According to this model, for a given material the

relative bulk modulus is proportional to the coordination number and the neck-to-particle radius ratio (r/R). By combining eqn (1) with the established relationships for neck growth, it is then possible to relate the elastic moduli of a porous material to the sintering mechanism.[2,7] For the case of alumina, the elastic constants were found to be consistent with the sintering mechanism of surface diffusion at the lower sintering temperatures and volume diffusion at the higher.[2] The increase in strength for alumina without any densification[6] is particularly intriguing, as it implies that one can control the strength of a porous material through manipulation of the sintering process.

In order to obtain further support for eqn (1), Nanjangud and Green[7] measured r/R for partially sintered glass spheres from observations of the fracture surface. The study demonstrated that a linear relationship between Young's modulus and the radii ratio was not unreasonable. Moreover, the study again showed that the elastic properties could be related to the sintering mechanism (viscous flow) and good agreement was obtained between the viscosity data obtained in this manner and previous literature data.[7] In order to understand the strength behavior of a porous material, information is needed on the fracture toughness behavior, and obtaining such data was the primary focus of the current study.

Mechanical property data on porous alumina has recently been gathered by Lam *et al.*[8] and they suggested the elastic constants and fracture toughness should be directly proportional to the degree of densification, i.e.

$$\frac{E}{E_0} = \frac{K_{IC}}{K_{IC}^0} = \left(1 - \frac{P}{P_I}\right) \tag{2}$$

where E and E_0 are the Young's modulus values of the porous and theoretically dense materials, respectively, K_{IC} and K_{IC}^0 are the fracture toughnesses of the porous and dense materials, respectively, P is the fractional porosity and P_I is the fractional porosity in the green state. By postulating an equation for the change in the crack size that initiates failure in these materials, Lam *et al.*[8] also put forward a theoretical relationship for the strength behavior of porous materials. Equation (2) clearly runs into difficulties for materials that undergo sintering without densification, and thus it was suggested recently[7] that the theory for the Young's modulus can be modified to

$$\left(\frac{E - E'}{E_0 - E'}\right) = \left(1 - \frac{P}{P_I}\right) \tag{3}$$

where E' is the Young's modulus at the onset of densification.

3 Experimental Procedure

Porous samples were processed by the partial sintering of powder compacts to various temperatures using a commercially available alumina (Malakoff Industries, TX., >99·99% purity, median particle size = 0·38 μm).

3.1 Sample processing

Bar specimens were used for the Young's modulus and fracture toughness determinations and ~10 individual bars were uniaxially dry-pressed at a pressure of 17 MPa for each batch. The specimens were also isostatically pressed to a pressure of 172 MPa. The specimen dimensions were typically 7 mm × 4 mm × 45 mm. The various batches of material were sintered to different temperatures ranging from 800 to 1600°C. The sintering was conducted in air with a heating rate of 10°C/min and a dwell time of 2 h at the maximum temperature. At the end of the isothermal hold, the samples were allowed to cool at a rate of about 5°C/min. Some isothermal sintering experiments were also conducted at temperatures of 900, 1050, and 1200°C for times up to 78 h.

Specimens for Young's modulus and strength testing were in the form of discs. Powder was introduced into a steel die with a diameter of 25·4 mm and uniaxially pressed to a stress of 45 MPa, but these samples were not isostatically pressed. The sintering procedure was identical to that for the bars. The densities of the bars and discs were both calculated from simple volume and mass measurements and the densities within the batches varied by less than 1%.

3.2 Young's modulus measurements

The Young's modulus of the bars was determined using a dynamic resonance technique from[9,10]

$$E = 0{\cdot}94642C\rho\left(\frac{L^2 f}{h}\right)^2 \tag{4}$$

where E is Young's modulus, L is the sample length, f is the fundamental flexural resonance frequency, h is the beam height, ρ is the density and C is a shape factor. The parameter C is dependent upon Poisson's ratio and values for a porous alumina were taken from a previous study.[2] This approach was considered to be acceptable as Poisson's ratio has only a small effect on the magnitude of C.

The Young's moduli of the discs were determined by an ultrasonic sound velocity technique. Longitudinal sound waves were transmitted through the thickness of the discs by means of a wave pulser and a 12·7-mm diameter, dry contact, 10 MHz transducer (Ultran Laboratories, Boals-

burg, PA). The transit-time measurement was made in the pulse-echo mode and E was calculated using

$$E = \frac{v^2[\rho(1 + \nu)(1 - 2\nu)]}{(1 - \nu)} \quad (5)$$

where v is the longitudinal sound velocity, ρ is density and ν is Poisson's ratio. The Poisson's ratio values for porous alumina were obtained from the literature.[2] Ten samples for each sintering temperature were measured, and the average Young's modulus values were calculated.

3.3 Strength testing

The strengths of the discs were measured using a 'piston on three ball' biaxial flexure test.[11] The load was applied using a commercial mechanical testing machine (Instron Corporation, Model 4200, Canton, MA.). The equation for calculating strength depends on Poisson's ratio, and again values were obtained from literature.[2] The fracture strength for each batch was taken as the average of the strengths of the individual samples. The discs broke into three or four pieces with the cracks originating from the center of the tensile side of the specimens.

3.4 Fracture toughness measurements

Fracture toughness values (K_{IC}) were measured using a four-point bend chevron-notch test.[12,22] This method was chosen to ensure the introduction of sharp cracks in these fragile porous materials. The details of the notching procedure are given elsewhere.[23] Fracture toughness values were determined using the analysis of Munz *et al.*[12] The major and minor spans of the bend fixture were 38·1 and 12·7 mm, respectively, and the crosshead speed was 0·05 mm/min. In the chevron-notch test, crack growth must proceed stably through the maximum load and the presence of stable crack growth was confirmed by the shape of the load–displacement curve obtained for each specimen. If stable growth occurred, the top of the curve would be rounded, whereas a catastrophic failure would give an instantaneous drop in load.

3.5 Microstructural characterization

Scanning electron microscope observations were made on planar sections of the samples to study the microstructural changes as a function of the degree of sintering. It is difficult to polish porous samples without damage, so vacuum impregnation with a cold-mounting epoxy (Epofix HQ, Struers, Westlake, OH) was used to fill the pores and strengthen the samples for polishing. The epoxy was heated to 50°C to reduce the viscosity, and then pieces of the broken discs were dropped into the epoxy in a vacuum chamber. The vacuum was released after 15–30 s to prevent the epoxy from vaporizing. The samples were then mounted for polishing in a different epoxy (M135 Fast Cure Epoxy, Metlab, Niagara Falls, NY). The infiltrated samples were polished to a 0·2-μm diamond paste finish. After polishing, the samples were heated on a hot plate and removed from the softened epoxy. The samples were then heated to 500°C to remove the infiltrated epoxy and, as a final step, were cleaned in acetone prior to microscopic observation.

4 Results and Discussion

Figure 1 shows the changes in the relative density of the alumina bars with sintering temperature. The densities of samples sintered to < 1100°C are relatively unchanged and densification occurs at the higher temperatures. The Young's modulus

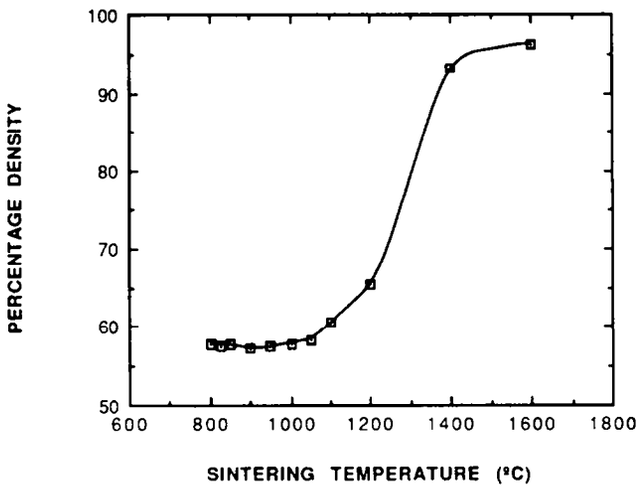

Fig. 1. Density of glass specimens after sintering at various temperatures, showing the onset of densification at ~1050°C.

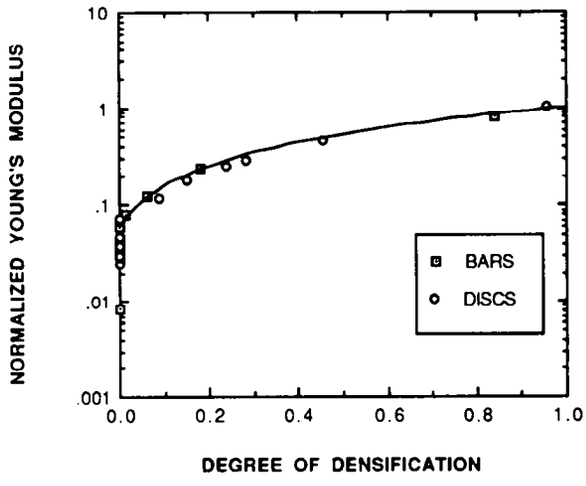

Fig. 2. Comparison of the room temperature Young's modulus values for porous alumina specimens after sintering to various temperatures as a function of the degree of densification with eqn (3).

data for the bars and discs are given as a function of the degree of densification in Fig. 2, i.e. $D = 1 - (P/P_I)$. As with the earlier studies,[2,6] there is a dramatic increase in the Young's modulus for specimens subjected to the initial stages of sintering with very little increase in density, reflecting neck growth by surface diffusion. It is also important to note the E data for both bars and discs fit a single function, even though there was a difference in their respective green densities, i.e. 58% and 54% theoretical density. In terms of eqn (3), the data show an excellent fit, using $E'/E_0 = 0{\cdot}06$. It would appear that the modification to eqn (2) is very useful, but it is still incapable of describing the changes in modulus that occurs for $D = 0$. For these cases, in which non-densifying sintering mechanisms are active, approaches such as that outlined in eqn (1) show more promise, but information on the changes in the r/R ratio and coordination number is difficult to obtain, especially when using sub-micrometer powder as a starting material.

Isothermal sintering was conducted at 900, 1050 and 1200°C and the Young's modulus data are shown in Fig. 3 as a function of the sintering time. For the 900°C and 1050°C sintering schedules, the modulus was substantially increased with no significant change in density (< 1%). This effect could be of technological interest in that Young's modulus can be doubled for this range of sintering times. For the 1200°C specimens, the modulus increased more dramatically, but the density was found to increase at a similar rate. As with the earlier study,[2] the variation in the elastic constants observed in the current study is consistent with a change in the dominant sintering mechanism, i.e. from surface diffusion to volume diffusion at ~1050°C.

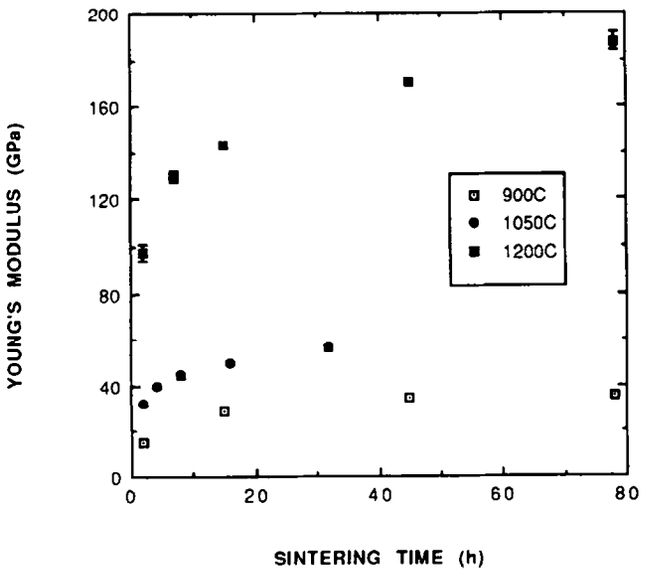

Fig. 3. Room-temperature Young's modulus values for porous alumina specimens after sintering at 900, 1050 and 1200°C for various times. These changes occur without significant densification at the two lower temperatures.

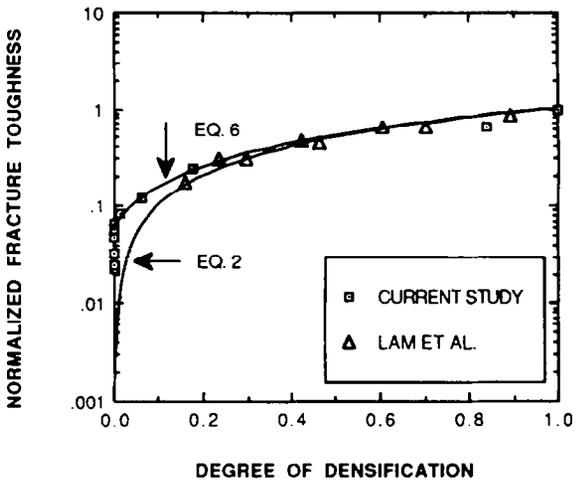

Fig. 4. Room-temperature fracture toughness values for porous alumina specimens after sintering to various temperatures as a function of the degree of densification. For small D, there is significant deviation from the theory of Lam *et al.*[8] Improved agreement is obtained using the proposed modification of eqn (6).

Mode I fracture toughness values (K_{IC}) are given as a function of D in Fig. 4 and are compared with eqn (2). The experimental data of Lam *et al.*[8] is also included in Fig. 4 and comparison with the theory for both data sets shows good agreement for $D \geq 0{\cdot}1$. The growth of the necks for $D = 0$ leads to a significant increase in fracture toughness and shows a strong similarity to the elastic constant data. For a density of 65·4% theoretical, the fracture toughness has increased to 1·06 MPa $\sqrt{m}$, which is a relatively significant value. To place this value in perspective, one should note that the value exceeds that of dense soda-lime-silica glass (~0·7 MPa $\sqrt{m}$). The discrepancy with eqn (2) for small D suggests that eqn (2) for fracture toughness could be modified in the same fashion as the equation for Young's modulus (eqn (3)), i.e.

$$\left(\frac{K_{IC} - K'_{IC}}{K^0_{IC} - K'_{IC}}\right) = \left(1 - \frac{P}{P_I}\right) \qquad (6)$$

where K'_{IC} is the fracture toughness at the onset of densification. The modification to the theory is shown in Fig. 4 using $K'_{IC}/K_{IC}{}^0 = 0{\cdot}06$, and the fit is excellent. A model has been developed that considers the fracture toughness of a partially sintered body in terms of particle neck failure.[23] Such a model would be supported by the increase in fracture toughness seen in Fig. 4 for $D = 0$, similar to the way in which the elastic data in Fig. 2 supports eqn (2). An important difference with the elastic problem is that failure may not necessarily pass through the interparticle necks.[7] For the current work, there was not enough direct evidence to test and support the model.

The biaxial flexural strengths of discs are plotted against relative density in Fig. 5. As with

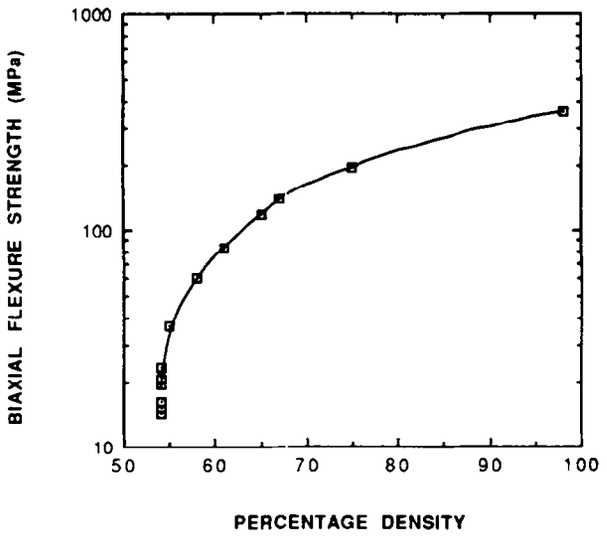

Fig. 5. Room-temperature biaxial flexure strength for porous alumina specimens after sintering to various temperatures as a function of the percentage theoretical density.

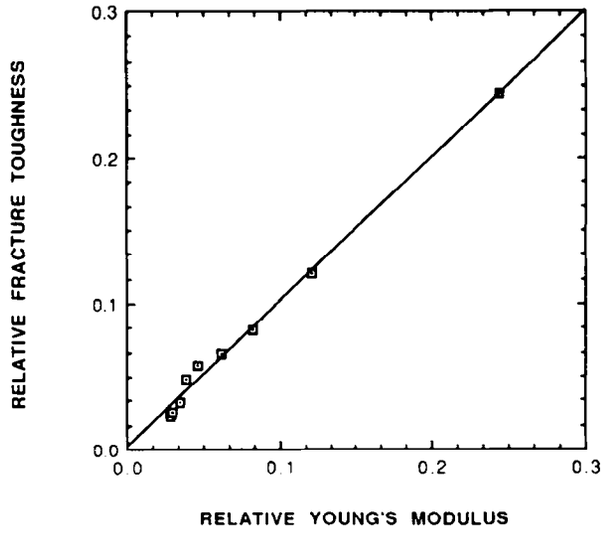

Fig. 6. Correlation between the relative Young's modulus and the relative fracture toughness for bar specimens.

Young's modulus and fracture toughness, there is a relatively large increase in strength for specimens sintered at temperatures below 1100°C. These data show that significant gains in strength of porous ceramics can be obtained with minimal densification. This flexural strength data, along with the Young's modulus and fracture toughness data, is very encouraging in that it demonstrates that the mechanical properties of a porous material can be enhanced at a particular density by control of the sintering mechanism.

The relationship between the strength of a brittle ceramic and its mode I fracture toughness is given as

$$\sigma_f = \frac{K_{IC}}{Y\sqrt{c}} \tag{7}$$

where σ_f is fracture strength, Y is a geometric constant and c is the critical crack length. Thus, the critical crack size can be calculated if σ_f and K_{IC} are known for a given material, and this gives insight into the failure process. In the present study, both σ_f and K_{IC} were measured, but not for the same sample geometry. The fracture toughness tests were conducted on bars, whereas discs were used for the biaxial flexure strength measurements. The difficulty in performing the crack size calculation was that the difference in specimen geometry for the toughness and strength tests gave rise to slight differences in green density. As Young's modulus was measured for both specimen types, it was postulated that K_{IC} could be empirically determined for the strength specimens from the correlation between K_{IC} and E. Equation (2) suggests that $(E/E_0) = (K_{IC}/K_{IC}^0)$ and as shown on Fig. 6, this approach gives a strong correlation even when $D = 0$. Higher-degree polynomials could be used in this fitting procedure, but this was found not to have a strong influence on the crack size calculation. Thus, the fracture toughness of the specimens used in the strength testing was estimated from the E values. The critical crack size, as calculated from eqn (5), is shown in Fig. 7 as a function of the sintering temperature. The value of $Y = 2/\sqrt{\pi}$ was used in the calculation, i.e. the value established for circular cracks of radius c. The critical crack size increased from about 45 to 70 μm as the degree of sintering progressed. At these high porosity levels, it is assumed that the major flaws are interconnected pores and it has been shown previously that pore sizes are expected to increase in alumina during the initial stages of sintering.[24] The data in Fig. 7 contrast strongly with the idea that the critical crack size decreases with increasing D, as suggested by Lam *et al.*[8] One suspects that the critical flaw evolution process may be rather complex and it may be

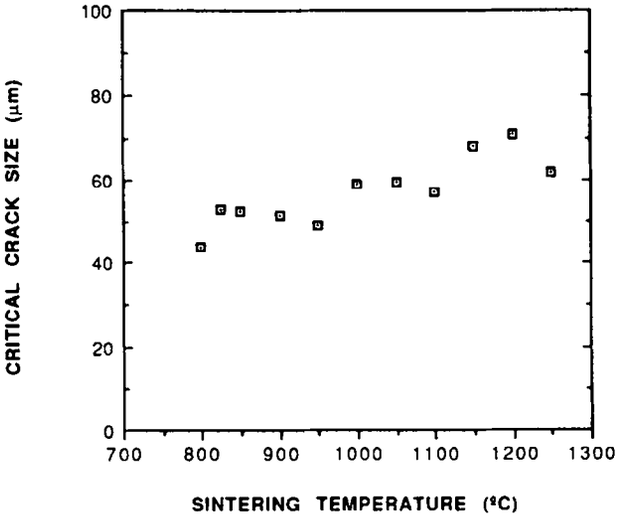

Fig. 7. Critical crack sizes calculated from the biaxial flexure strength and estimated fracture toughness data, assuming a circular flaw geometry, as a function of the sintering temperature.

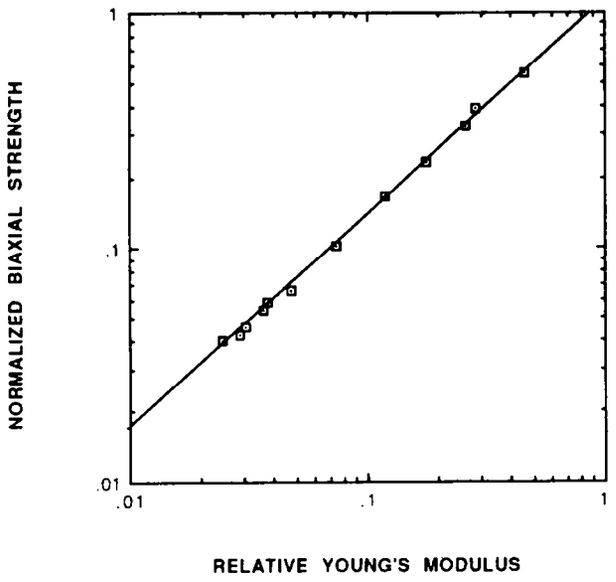

Fig. 8. Empirical correlation between biaxial flexure strength and relative Young's modulus. The strengths were normalized by the strength at the highest density, 357 MPa.

preferable to measure both strength and fracture toughness and obtain empirical information on the changes in critical crack size. For the current work, the critical crack sizes show a fairly smooth variation with increased sintering and as there is a strong correlation between fracture toughness and Young's modulus, one also finds a strong correlation between strength and Young's modulus, as shown in Fig. 8.

Figure 9 shows micrographs for samples sintered at 800, 1000, 1100 and 1200°C. Up to 1050°C, there is no obvious change in particle size or coordination, but some neck growth can be discerned. Above 1050°C, the increased density of the structure becomes apparent as clusters of particles coalesce into a chain-like morphology.

5 Summary and Conclusions

The Young's modulus, strength and fracture toughness of alumina with moderate amounts of porosity (~20–40%) showed similar behavior as a function of the degree of sintering. For low sintering temperatures (< 1050°C), these mechanical properties change with only minimal densification and this was considered to be due to neck growth by surface diffusion. At these temperatures, increases in sintering time can also be used to increase Young's modulus. Modifications to a recent theory that considers the relative Young's modulus and relative fracture toughness to be dependent upon the degree of densification showed very good agreement with the experimental data after densification had initiated. For the present

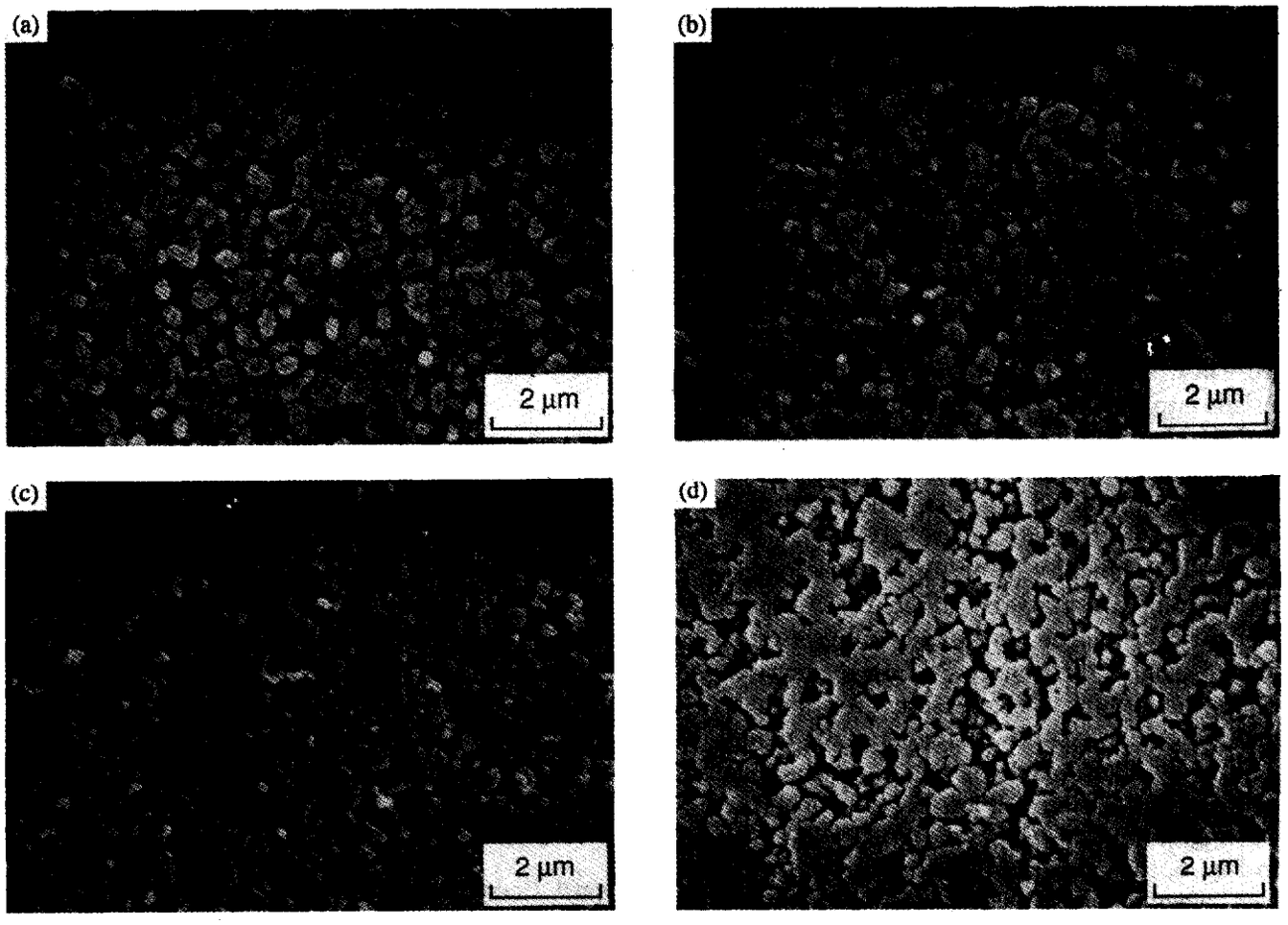

Fig. 9. Scanning electron micrographs showing specimens sintered at (a) 800°C, (b) 1000°C (c) 1100°C and (d) 1200°C.

study, the critical crack size in these porous materials was found to increase slightly as the sintering temperature was increased. Overall, this work shows that significant improvements in the mechanical properties of porous ceramics can be obtained by control of the sintering process and in some cases, with minimal densification.

Acknowledgement

The authors would like to acknowledge the National Science Foundation for financial support under Grant No. DMR. 8818908.

References

1. Green, D. J., Brezny, R. & Nader, C., The elastic behavior of partially-sintered ceramics. In *Adhesion In Solids*, MRS Symposium Proceedings, Vol. 119, eds. D. M. Mattox, J. E. E. Baglin, R. J. Gotschall & C. D. Batich. Materials Research Society, Pittsburgh, PA, 1988, pp. 43–8.
2. Green, D. J., Nader, C. & Brezny, R., The elastic behavior of partially-sintered alumina. In *Sintering of Advanced Ceramics*, eds. C. A. Handwerker, J. E. Blendell & W. Kaysser. American Ceramic Society, Westerville, OH, 1990, pp. 347–56.
3. Woignier, T. & Philippou, J., Mechanical strength of silica aerogels. *J. Non-Cryst. Solids*, **100** (1988) 404–8.
4. Kendall, K., Alford, N. McN. & Birchall, J. D., Elasticity of particle assemblies as a measure of the surface energy of solids. *Proc. R. Soc., Lond., A*, **412** (1987) 269–83.
5. Cytermann, R., A new way of investigating the dependence of elastic moduli on the microstructure of porous materials. *Powder Metall Int.*, **19** (1989) 27–30.
6. Nanjangud, S. C., Brezny, R. & Green, D. J., Strength behavior of a partially-sintered alumina. *J. Am. Ceram. Soc.*, **78** (1995) 266–8.
7. Nanjangud, S. C. & Green, D. J., Mechanical behavior of porous glasses produced by sintering of spherical particles. *J. Eur. Ceram. Soc.*, in press.
8. Lam, D. C. C., Lange, F. F. & Evans, A. G., Mechanical properties of partially dense alumina produced from powder compacts. *J. Am. Ceram. Soc.*, **77** (1994) 2113–17.
9. Davis, W. R., Measurement of the elastic constants of ceramics by resonant frequency methods. *Trans. Br. Ceram. Soc.*, **67** (1968) 515–41.
10. Spinner, S. & Tefft, W. E., A method for determining mechanical resonance frequencies and for calculating elastic moduli from these frequencies. *Proc. ASTM*, **61** (1961) 1221–38.
11. Standard test method for biaxial flexure strength (modulus of rupture) of ceramic substrates. *ASTM F*, **394–78** (1978) 313–17.
12. Munz, D. G., Shannon, J. L. & Bubsey, R. R., Fracture toughness calculation from maximum load in four point bend tests of chevron notch specimens. *Int. J. Fracture*, **16** (1980) R137–41.
13. Bluhm, J. I., Slice synthesis of a three dimensional 'work of fracture' specimen. *Engng. Fract. Mech.*, **7** (1975) 593–604.
14. Munz, D., Bubsey, R. T. & Shannon, J. L. Jr., Fracture toughness of Al_2O_3 using four-point-bend specimens with straight-through and chevron notches. *J. Am. Ceram. Soc.*, **63** (1980) 300–5.
15. Brown, K. R., The chevron notched fracture toughness test, a convenient and inexpensive test at long last. *ASTM Standardization News*, **Nov.** (1988) 66–9.
16. Reddy, K. P. R., Fontana, E. H. & Helfinstine, J. D., Fracture toughness measurement of glass and ceramic materials using chevron-notched specimens. *J. Am. Ceram. Soc.*, **71** (1988) C310–13.
17. Munz, D., Effect of specimen type on the measured values of fracture toughness of brittle ceramics. In *Fracture Mechanics of Ceramics*, Vol. 6, eds. R. C. Bradt, A. G. Evans, D. P. H. Hasselman & F. F. Lange. Plenum Press, New York, 1983, pp. 1–25.
18. Shannon, J. L. Jr. & Munz, D. G., Specimen size and geometry effects on fracture toughness of aluminum oxide measured with short-rod and short-bar chevron-notched specimens. In *Chevron-Notched Specimens: Testing and Stress Analysis*, ASTM STP 855, eds. J. H. Underwood, S. W. Freiman & F. I. Baratta. ASTM, Philadelphia, 1984, pp. 270–80.
19. Bluhm, J. I., Stability considerations in the generalized three dimensional 'work of fracture' specimen. In *Fracture*, Vol. 3. ICF4, Waterloo, Canada, 1977, pp. 409–17.
20. Chuck, L., Fuller, E. R. Jr. & Freiman, S. W., Chevron-notch bend testing in glass: some experimental problems. In *Chevron-Notched Specimens: Testing and Stress Analysis*, ASTM STP 855, eds. J. H. Underwood, S. W. Freiman & F. I. Baratta. ASTM, Philadelphia, 1984, pp. 167–75.
21. Shang-Xian, W., Compliance and stress-intensity factor of chevron-notched three-point bend specimen, *ibid.*, pp. 176–92.
22. Munz, D., Bubsey, R. T. & Shannon, J. L. Jr., Performance of chevron-notch short bar specimen in determining the fracture toughness of silicon nitride and aluminum oxide. *J. Test. Eval.*, **8** (1980) 103–7.
23. Hardy, D., Mechanical properties of partially sintered alumina. MS Thesis, The Pennsylvania State University, 1992.
24. Whittemore, O. J. & Sipe, J. J., Pore growth during the initial stages of sintering ceramics. *Powder Technol.*, **9** (1974) 159–64.